Strain hardening behavior of ARMCO iron processed by ECAP

2014 IOP Conf. Ser.: Mater. Sci. Eng. 63 012143

(http://iopscience.iop.org/1757-899X/63/1/012143)

IOP Conf. Series: Materials Science and Engineering **63** (2014) 012143 doi:10.1088/1757-899X/63/1/012143

Strain hardening behavior of ARMCO iron processed by ECAP

J A Muñoz Bolaños[1], O F Higuera Cobos[2] and J M Cabrera Marrero[1, 3]
[1] Department of Materials Science and Metallurgical Engineering ETSEIB, Universidad Politecnica de Catalunya, Av Diagonal 647, 08028 Barcelona, Spain.
[2] Faculty of Mechanical Engineering, Universidad Tecnológica de Pereira, Colombia.
[3] Fundación CTM, Plaça de la Ciència, 2, 08243, Manresa, Spain.
E-mail: jairomunoz8614@gmail.com

Abstract. The strain hardening behavior of an ARMCO iron processed by ECAP at room temperature up to sixteen passes following route Bc was investigated through Hollomon and differential Crussard-Jaoul models. Results indicate that the Hollomon analysis shows some deviations from the experimentally determined true stress - true strain curves while the differential Crussard-Jaoul analysis based on the Ludwik equation and the modified Crussard-Jaoul analysis based on the Swift equation fit better when two work hardening exponents are considered. As expected, the strength of the material increased with the number of ECAP passes. Indeed the ultimate tensile stress reached a maximum of ~900MPa after 16 passes, which is more than three times higher than the UTS of the annealed material. Nevertheless, the strain hardening capacity of the material was reduced in comparison with the material without severe plastic deformation. For that reason the tensile ductility was also reduced at increasing ECAP passes. The increase in strength was attributed to the reduction of the grain size through refined sub-grains with high density of dislocations. After sixteenth passes the original grain size (namely 70 mm) was reduced down to 300 to 400 nm observing a good correspondence with the Hall-Petch relationship. The microstructural analysis, carried out by EBSD, showed an increasing amount in the fraction of high Angle Grain Boundaries (HAGB) after 1 pass due to the regeneration of the microstructure with a smaller grain size.

Keywords: ARMCO iron, ECAP, Hollomon, Crussard-Jaoul, LAGB, HAGB.

1. Introduction

Over the past few years, tailoring microstructures with ultrafine grain sizes in bulk materials has attracted significant interest from the scientific community. This is due to the fact that grain size strengthening is one of the few mechanisms that lead to improvement in the strength of materials, retaining an appreciable level of ductility and flow properties. Ultrafine grain sizes in bulk materials can be achieved by Severe Plastic Deformation (SPD), which involves extremely large imposed plastic strains without significant change of dimensions of the workpiece [1]. However, in general, UFG materials have an inherent mechanical drawback, i.e., a lack of strain hardening, resulting from the fact that the grain size is comparable to the dislocation cell size which corresponds to the dislocation mean free length [2]. The aim of this study is to characterize the microstructure and mechanical properties of iron after severe plastic deformation at room temperature (SPD) via the equal channel angular pressing (ECAP) method.

2. Experimental procedure

A commercial ARMCO iron (Fe-0.01%C-0.01%Si-0.059%Mn-<0.01%P-<0.010%S-0.02%Cr-<0.005%Mo-0.038%Ni-0.013%Al (in wt %))was received in the form of rods, then divided into short billets having lengths of ~60mm, which were subjected to severe plastic deformation using ECAP at room temperature. Before pressing, samples were annealed at 1203K during 20 minutes in a tubular radiation heat furnace with a protective inert atmosphere of argon. Following annealing, samples were severely deformed at room temperature by ECAP to a maximum equivalent strain of sixteen (N=1, 4, 8 and 16 passes) following route Bc. ECAP was carried out using a solid die fabricated from insert tool steel with two channels intersecting at an inner angle of $\Phi = 90^{o}$ and an outer angle of $\psi = 37^{o}$, resulting in a strain of ~1 per pass. To evaluate the mechanical properties of the ECAPed

material, tension tests at room temperature were performed using an INSTRON 5585 H universal testing machine equipped with a video camera extensometer. Tensile specimens were tested at a constant crosshead velocity of $3.3*10^{-3}$ mm/s until failure. The microstructure of the samples was characterized by Electron Backscattered Diffraction (EBSD). Specimens were cut from the centre of the ECAP samples and mechanically polished following standard metallographic procedures. Three empirical fitting equations (Hollomon [18], Ludwik [19] and Swift [20]) and the mathematical analyses (Hollomon [18], Crussard-Jaoul [21, 22] and modified Crussard-Jaoul [23]) based on these equations was used. These analyses assume that the true stress and true strain are expressed in the form of a power relationship which gives a measure of strain hardening capability. The power relationships are:

Hollomon equation: $$\sigma = k_H \varepsilon^{n_H} \quad (1)$$

Here the n_H and k_H are obtained from the slope and intercept of a $ln\ \sigma$-$ln\ \varepsilon$ plot respectively.

Ludwik equation: $$\sigma = \sigma_0 + k_L \varepsilon^{n_L} \quad (2)$$

Where σ_o is the yield stress, k_L is the strength coefficient and n_L the work hardening exponent. To determine significant variations of the work hardening exponent, the logarithmic form of equation (2), after differentiation with respect to ε, formally establishes the Crussard-Jaoul (C-J) analysis method [24-27]:

$$\ln\left(d\sigma/_{d\varepsilon}\right) = (n_L - 1) ln\varepsilon + \ln\,(k_L n_L) \quad (3)$$

In a $ln\ (d\sigma/d\varepsilon) - ln\ \varepsilon$ plot, the slope of the line gives $(n_L\text{-}1)$, and its intersection with $ln\ \varepsilon = 0$ provides $ln\ (k_L n_L)$.

Swift equation: $$\varepsilon = \varepsilon_0 + k_S \sigma^m \quad (4)$$

The modified differential Crussard-Jaoul analysis takes the logarithmic form of equation (4), after differentiation with respect to ε, so that the strain hardening exponents can be obtained by a linear regression as in the differential Crussard-Jaoul analysis.

$$\ln\left(d\sigma/_{d\varepsilon}\right) = (1 - m) ln\sigma + \ln\,(k_S m) \quad (5)$$

3. Results and discussion

3.1. Microstructure

The microstructure of the unprocessed annealed iron consists of equiaxed grains with an average size of 72μm characterized mainly by High Angle Grain Boundaries (HAGB), due to the complete recrystallization of the material as shown in Figure 1a. After the first pass the microstructure became reoriented and shear strained (Figure 1b) with a high fraction of Low Angle Grain Boundaries (LAGB) with an average grain size of 1.89μm. In the initial stage of SPD processing, geometrical necessary boundaries are formed to subdivide the coarse grains into cell blocks [11]. For that reason in the first pass one finds a high fraction of LAGB while in the following passes (4, 8 and 16 passes) HAGB increase in quantity continuously (Figure 2a).

After four and eight passes the microstructure becomes smaller and equiaxed with an increment in the HAGB with respect to the material with one pass, promoting grain sizes of

435nm and 365nm respectively. Finally after sixteen passes the material has the highest fraction of HAGB (Figure 2a) since the microstructure is almost totally formed by equiaxed grains with an average grain size of 275nm. Thus the microstructure has been totally regenerated with a smaller grain size. In Figure 2b we have a comparison of Hall-Petch relationship between our iron and some low carbon steels deformed by others techniques of SPD and by conventional methods of deformation, it can be seen how the points after 8 and 16 passes are very close to the points of deformed steels. This confirms that there was a great reduction in the grain size.

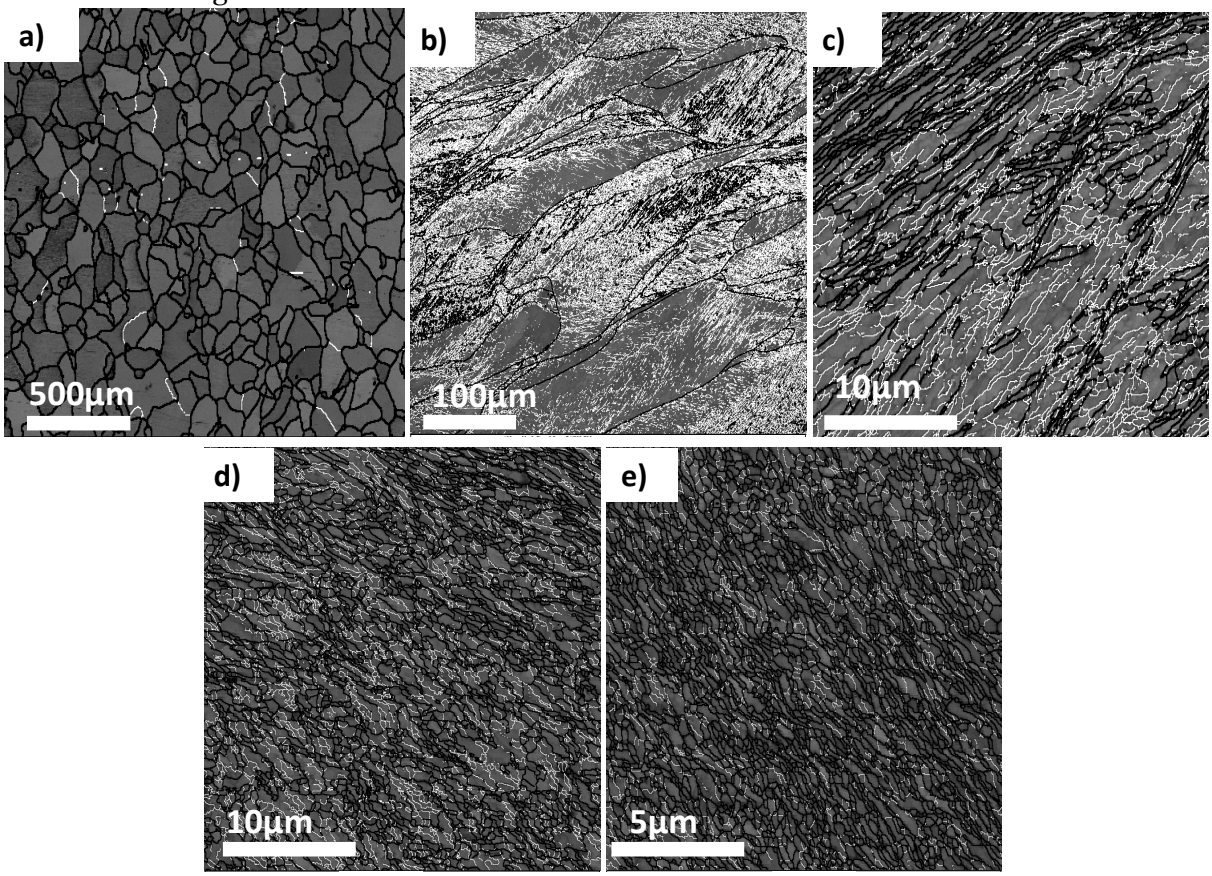

Figure 1. EBSD microstructure characterization. (a) As-received; (b) After 1 pass; (c) after 4 passes; (d) after 8 passes; and (e) after 16 passes.

3.2. Mechanical properties

The effect of multi-pass ECAP on the mechanical properties at room temperature, as plotted in the form of engineering stress- strain and true stress- strain curves is shown in Figure 3a. Firstly it is observed that the annealed sample showed extended uniform deformation (~22%) with respect to the material deformed by ECAP (less than 4% for all the passes).

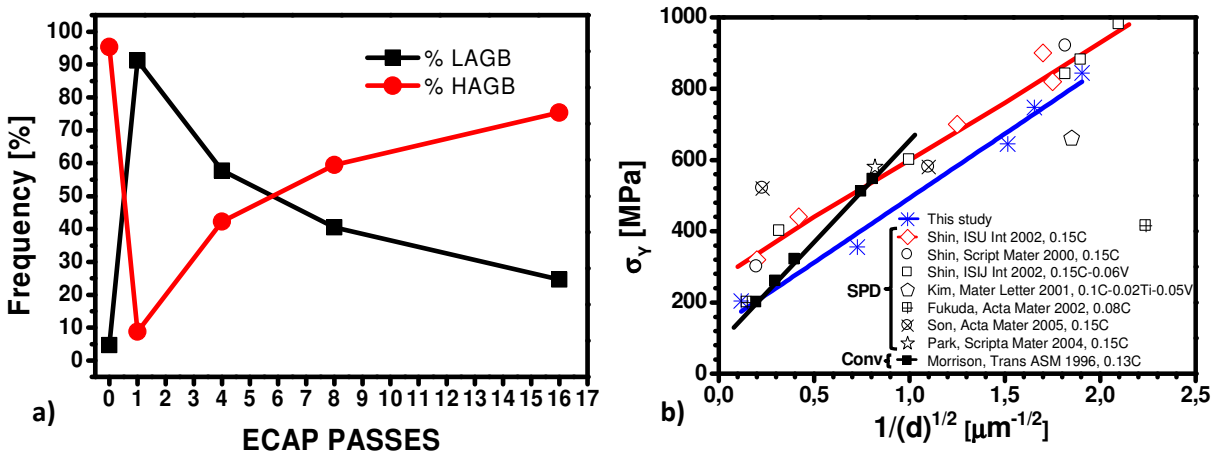

Figure 2. Microstructure nature. (a) Microstructure properties; (b) Hall-Petch relationship.

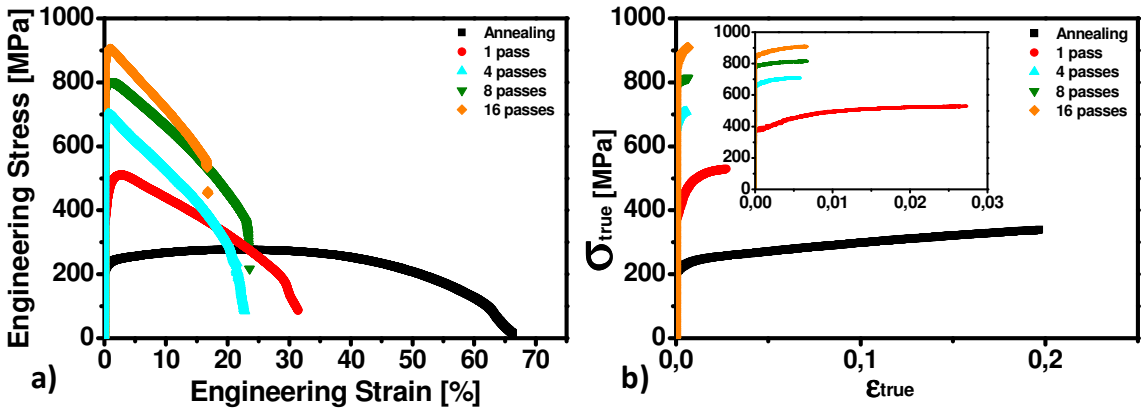

Figure 3. Tensile curves. (a) Engineering stress-strain curves; (b). True stress-strain curves.

In general, the engineering stress-strain curves of the deformed material showed the maximum strength at the early stage of deformation, followed by a region of plastic instability until failure. This softening is associated to the necking occurrence during the tensile test. The yield stress σ_y, the ultimate tensile strength σ_{UTS} and the uniform deformation for the as annealed material are 204MPa, 277MPa and 22.49% respectively. After four ECAP passes, a strong increase in strength (σ_y = 645MPa, σ_{UTS} = 700MPa) with a significant decrease in ductility was observed. Similar values of yield stress and strength were reported for Gang et al [5] in an iron with 99.86% Fe processed up to four passes. Nevertheless a slight increment in uniform elongation is noticed after the fourth pass as shown in Figure 3b.. It is also important to notice that material with sixteen passes present an increment of ~3 times in strength with respect to the annealed one reaching 904MPa which is quite similar to the values reported for low carbon steels processed by ECAP by Park et al [6]. These authors found a strength of ~900MPa for a low carbon steel (Fe-0.15%C-0.25Si-1.1%Mn(in wt%)) processed up to four passes via route C at 500°C. On the other hand Ding et al [7] got strength of 680 MPa in pure iron processed by asymmetric rolling (ASR) with a prevalence of HAGB.

3.3. Strain hardening behavior

One of the mechanical characteristics of iron processed by ECAP is the lack of ductility. Since strain hardening is directly associated with formability, the study of strain hardening behavior is quite important to establish the responsible mechanisms of this phenomenon.

Three analyses (Hollomon, C-J and modified C-J) were applied to the stress-strain data of the present steels and the results are shown in Figures 4a, 5a and 6a. Figure 7 shows a comparison of the parameters obtained applying these three methods. Finally to evaluate the results of these methods of analysis, the calculated and experimental true stress-strain curves have been redrawn in Figures 4b, 5b and 6b. As shown in Figure 4a, the Hollomon analysis shows a good agreement to the experimental data especially for the material with 8 and 16 passes. On the other hand the differential C-J model and the modified differential C-J model which are more sensitive to slope changes in the true stress-strain curve fits better to the experimental data. It has been reported that the modified C-J analysis is more sensitive to microstructures than the other two and able to distinguish the different stages of strain hardening of Al, Cu and steels with different microstructures. [29-31]. With respect to the Hollomon analysis it can be seen how the strain hardening coefficient n_H increases until the first pass due to the great presence of dislocations generated by the deformation introduced. After the 4th pass the value of n_H decreases drastically as shown in Figure 7. This observation is in correspondence with the fact that the uniform plastic zone in the sample with 4 passes is the smallest, this could be attributed to the presence of a heterogeneous microstructure (combination of HAGB and LAGB) besides the fact that there is a considerable reduction in the grain size, which means less freedom for the dislocations movement. For the 8th and 16th passes there is a small increase in n_H coefficient with the tendency to stabilize around 0.02. This slight growth can be attributed to the new change in the microstructure nature, because a higher fraction of HAGB than LAGB (Figure 2a) is obtained due to the microstructure evolution during the ECAP passes. The present values are quite similar to the values reported by Mejia et al [28] for cold worked steel with 0.18%C. The differential C-J and modified C-J analysis show clearly that the flow curves can be divided in two stages. The values of n_L and $1/m$ are significantly smaller in the second part of the flow curve than in the first part. These results also agree with the values obtained by Mejía et al [28]. Both models show growing values of n_L and $1/m$ with the number of ECAP passes for the first stage, suggesting that strain hardening in the initial stage is carried out faster in the material. However in the second stage there is a tendency to decreases until the 4th pass, with a subsequent increase and stabilization for the 8th a 16th passes. This could be attributed to the simultaneous occurrence of dislocation multiplication and annihilation which eventually leads to a saturation of the dislocation density. Under such conditions the flow stress should saturate as well [32]. Indeed, Mecking et al. [33] have interpreted the fairly general observation that the rate of work hardening decreases continuously at high strains, in terms of an asymptotic saturation of the flow stress. Similar values of m also were found by Huang et al [34] in copper processed by ECAP after 16th passes following the modified C-J analysis. They established five stages of deformation in Cu, where only stages IV and V are presented in Cu after ECAP. Huang et al [34] said that stage IV is governed by athermal dislocation storage, whereas the stage V is characterized by thermally activated recovery process, i.e., the equilibrium between generation and annihilation of dislocations [35, 36]. They attributed the apparition of a steady state flow stress to the extensive recovery of dislocations in the stage V. In the case of UFG Cu, the mechanism of strain hardening in the first stage could stem from that there is a limited space in grains allowing certain storage of dislocations. Accordingly, a fast increase of flow stress can be observed in the early stage of plastic strain. However, it cannot be expected that the strain hardening in this stage could sustain a large plastic strain because of the low efficiency of dislocation storage inside small grains at room temperature. After that, a stage of softening process resulted from dynamic recovery takes place and the

flow stress increases very slowly until necking occurred. As a consequence, due to the limited capability of strain hardening in the first stage plus subsequent softening process in the second stage, UFG Cu exhibited only small uniform plastic strain . This has been confirmed not only in UFG Cu, but also in many other UFG metals, such Ti and Ni [37,38].

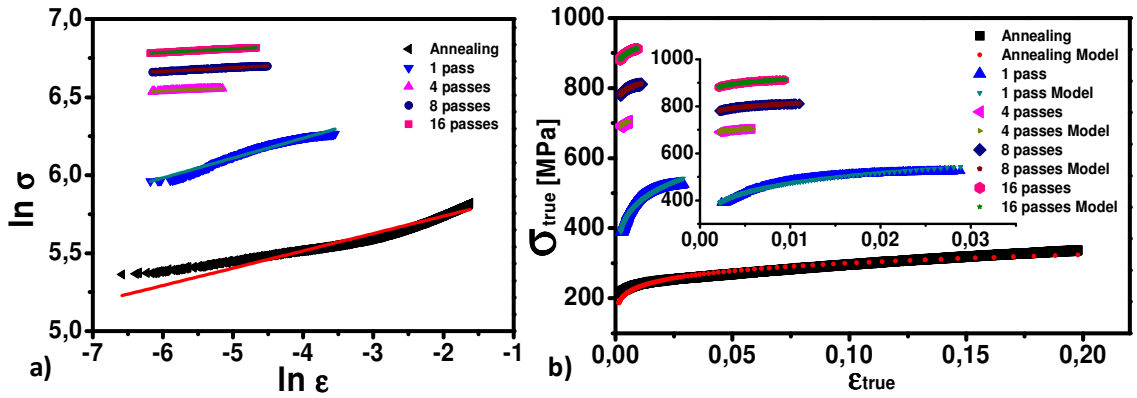

Figure 4. Hollomon analysis. (a) Hollomon's fit ; (b) application of the Hollomon analysis to the experimental data.

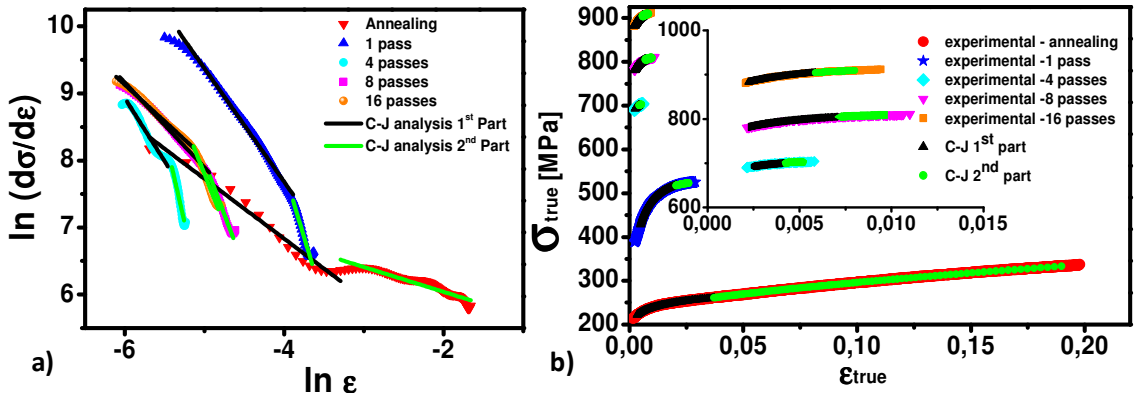

Figure 5. C-J analysis. (a) C-J analysis's fit; (b) application of the C-J analysis to the experimental data.

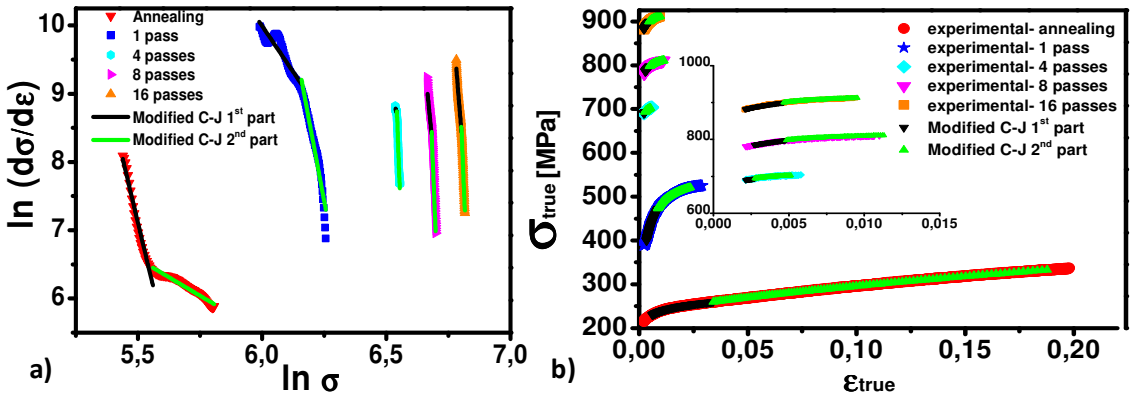

Figure 6. Modified C-J analysis. (a) Modified C-J analysis's fit; (b) application of the modified C-J analysis to the experimental data.

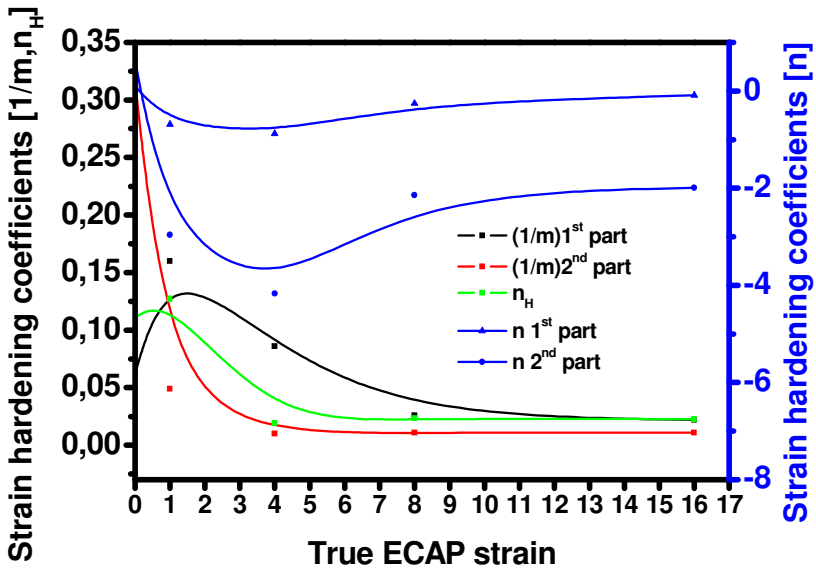

Figure 7. Strain hardening coefficients after the three different analysis.

4. Conclusions

The main conclusions of this study can be summarized as follows:

1. A great reduction in the grain size with the prevalence of HAGB was obtained in ARMCO iron after processing by ECAP up to 16 passes following route B_C at room temperature.
2. The strength of the material increased with the number of ECAP passes. The ultimate tensile stress reached a maximum of ~900MPa after 16 passes, which is more than three times higher as compared to that of the as received material. Nevertheless, the strain hardening capacity of the material was reduced in comparison with the material without ECAP. For that reason the tensile ductility was also reduced. The increase in strength was attributed to the reduction of the grain size through refined sub-grains with high density of dislocations.
3. The loss of strain hardening capacity was studied using three different analyses based in three equations (Hollomon, Ludwik and Shift). Hollomon analysis shown that the strain hardening coefficient n_H decreases after the first pass by one magnitude order, which indicates the material almost has lost the strain hardening capacity. Additionally to the Hollomon analysis, the C-J and modified C-J analyses allow to understand there are two stages of deformation, the first one characterized by a higher strain rate hardening than the second one. The opposite happens in the annealed condition. The second stage hardening stage of deformation in iron processed by ECAP is characterized by a smaller strain rate hardening which presents flow stress saturation.

Acknowledgements

Jairo Alberto Muñoz Bolaños thanks the funding and technical support received through Spanish education ministry with the FPU scholarship, and from Fundació CTM Centre Tecnologic respectively.

References

[1] Zehetbauer M J 2009 Bulk Nanostructured Materials, *Wiley-VCH*
[2] Son Y I, Lee Y K, Park K-T, Lee C S and Shin D H 2005 *Acta Materialia* **53** 3125–3134
[3] Hollomon J H 1945 *Trans Metall Soc AIME* 162:268
[4] Ludwik P 1909 Elemente der technologishen mechanik Berlin: *Springer*; p. 32

[5] Swift H W 1952 *J Mech Phys Solids*; **1**:1
[6] Crussard C 1950 *Rev Metall*; **47**:589
[7] Jaoul B J 1957 *Mech Phys Solids*; **5**:95
[8] Reed-Hill R E, Cribb W R and Monteiro S N 1973 *Metall Trans*; **4**:2665
[9] Ramos L F, Matlock D K and Krauss G 1979 *Metall. Trans*. A Vol. **10A** p.259
[10] Nagorta M S, Krauss G and Matlock D K 1987 *Mater. Sci. Eng*. *A* Vol. **94** p.183
[11] Tomita Y and Okabayashi K 1985 *Metall. Trans*. *A* Vol. **16A** p. 865
[12] Jiang Z, Lian J and Chen J 1992 *Mater. Sci. Tech*. Vol. **8** p. 1075
[13] Bay B, Hansen N, Hughes D A and Kuhlmann-Wilsdorf D 1992 *Acta Metal. Mater*. **40** 205–219
[14] Fukuda Y, Oh-Ishi K, Horita Z and Langdon T G 2002 *Acta Mater*. **50** 1359
[15] Son Y I, Lee Y K, Park K.-T, Lee C.S and Shin D H 2005 *Acta Mater*. **53** 3125
[16] Park K-T, Han S Y, Ahn B D, Shin D H, Lee Y K and Um K K 2004 *Scripta Mater*. **51** 909
[17] Kim W J, Kim J K, Choo W Y, Hong S I and Lee J D 2001 *Mater. Lett*. **51** 177
[18] Shin D H, Park J-J, Chang S Y, Lee Y-K and Park K-T 2002 *ISIJ Int*. **42** 1490
[19] Shin D H, Seo C W, Kim J, Park K-T and Choo W Y 2000 *Scripta Mater*. **42** 695
[20] Morrison W B 1966 *Trans. ASM* **59** 824
[21] Gang Y, Mu-xin Y, Zheng-dong L and Chang W 2011 *Journal of Iron and Steel Research*. **18**(12). 40-44
[22] Park K-T, Han S Y, Ahn B D, Shin D H, Lee Y K and Um K K 2004 *Scripta Materialia* **51** 909–913
[23] Ding Y, Jiang J and Shan A 2009 *Materials Science and Engineering A* **509** 76–80
[24] Reed-Hill R E, Gribb W R and Monteiro S N 1973 *Metall. Trans*. **4**, 2665
[25] Tomita Y and Okabayashi K 1985 *Metall. Trans*. *A* **A16**, 865
[26] Son Y II, Lee Y K, Park K T, Lee C S and Shin D H 2005 *Acta Mater*. **53**, 3125
[27] Mejía I, Maldonado C, Benito J A, Jorba J and Roca A 2006 *Mater. Sci. Forum*. Vol. **509** p. 37.
[28] Essman U and Mughrabi H 1979 *Philosophical Magazine A*, **40** (6) p. 731
[29] Mecking H, Kocks U F and Fischer H 1976 *Proceedings of the Fourth International Conference on the Strength of Metals and Alloys*, Nancy, Vol. **1**, p. 334.
[30] Huang C, Wu S, Li S and Zhang Z 2008 *Adv. Eng. Mater*., vol. **10**, pp. 434 438
[31] Zehetbauer M and Seumer V 1993 *Acta Metall. Mater*. **2**, 577
[32] Les P, Zehetbauer M, Rauch E F, Kopacz I 1999 *Scr. Mater*. **41**, 523
[33] Jia D, Wang Y M, Remesh K T, Ma E, Zhu Y T and Valiev R. Z 2001 *Appl. Phys. Lett*. **79**, 611.
[34] Gu C D, Lian J S, Jian Z H and Jiang Q 2006 *Scr. Mater*. **54**, 579
[35] Hirsch P B 1968 *Trans. Jap. Inst. Metals, Suppl*., **9**, xxx
[36] Šesták B, and Seeger A 1971, *Phys. Stat. Sol*. (b), **43**, 433
[37] Lawley A and Gaigher H L 1964, *Phil. Mag*., **10**, 15
[38] Solomon H D and Mcmahon C J, JR 1968, Work Hardening, edited by J. P. Hirth and J. W. Weertman (New York : Gordon & Breach), p. 311